JTTEE5 15:524-530
DOI: 10.1361/105996306X147306
1059-9630/$19.00 © ASM International

Peer Reviewed

Modeling the Restrike Mode Operation of a DC Plasma Spray Torch

E. Moreau, C. Chazelas, G. Mariaux, and A. Vardelle

(Submitted February 26, 2006; in revised form April 19, 2006)

A key aspect of the operation of conventional non-transferred direct current (dc) plasma torches is the random motion of the arc inside the nozzle. Various plasma gun designs have been developed to limit the arc fluctuations without increasing the heat load to the anode wall that results in surface erosion and anode wear. However, construction of these plasma torches is highly complex, while the conventional dc plasma torch consists of a small number of elements and is simple to manufacture and maintain. A better understanding of the behavior of the arc-anode attachment and how it depends on operating conditions may help in the design and operation of conventional plasma torches so that the fluctuation of the time-voltage, and therefore the time-enthalpy variation, is as low as possible with a fluctuation frequency adapted to the time characteristic of the powder particles in the plasma jet. This study deals with a three-dimensional (3D) time-dependent modeling of the arc and plasma generation in such a torch operating under the so-called "restrike" mode. The latter is characterized by rather large voltage fluctuations, corresponding to a broad range of conditions used in the manufacturing of plasma coatings. The mathematical model is based on the simultaneous solution of the conservation equations of mass, momentum, energy, electric current, and electromagnetic equations. These make it possible to predict the effect of operating parameters of the plasma torch on the motion of the anode root attachment over the anode surface and the time-evolution of arc voltage and flow fields in the nozzle.

Keywords electric arc, plasma spraying, plasma torch, 3-D modeling, transient modeling

1. Introduction

The direct current (dc) plasma torch is used predominantly for plasma spraying of coatings. The conventional torch is characterized by a simple design involving a rod-shape cathode and a concentric water-cooled anode. The arc strikes from the tip of the cathode to some point on the anode wall where it attaches in the form of a high-temperature, low-density gas column cutting through the cold gas boundary layer that covers the anode wall (Fig. 1). As observed experimentally (Ref 1-3), the thickness of this boundary layer, which behaves as an electrically insulating layer enveloping the arc, controls the operation mode of the torch and depends on the plasma torch working parameters: principally, the inner diameter of the exit nozzle, the arc current intensity, and the plasma gas flow rate. The arc attachment is perpendicular to the anode surface and is subjected to a pulling down drag force exerted by the cold flow in the boundary layer and the Lorentz forces due the self-magnetic fields induced by the curvature of the current flow. The Lorentz forces may act in the same or opposite direction as the flow drag force depending on the curvature of the current lines in the anode arc root. Under the combined action of these forces, the anode arc attachment will generally exhibit an axial and rotational movement on the anode surface. The latter is favored by the symmetry of the torch design, as no particular point on the anode wall can be said to be, a priori, preferred for the arc attachment. This rotational motion is also strongly favored by the vortex injection of the plasma-forming gas. The axial displacement of the arc root brings about a variation in the length of the arc column and, therefore, in enthalpy input to the gas, while the rotational movement does not affect the latter. However, rotational displacement results in a nonsymmetry in the gas flow field and, consequently, inhomogeneity in the plasma jet issuing from the plasma torch.

Due to the design of the conventional plasma spray torch and its mode of operation, there are arc instabilities and it is necessary to control the residence time of the arc at a given location to

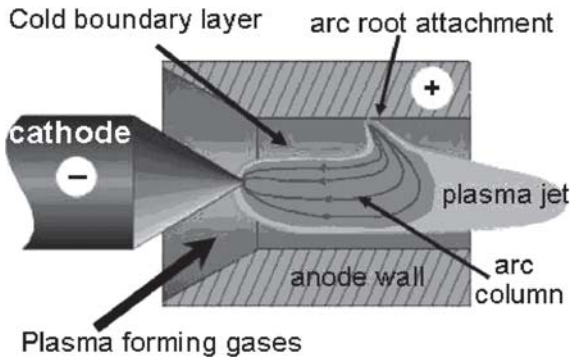

Fig. 1 Schematic representation of a non-transferred dc plasma torch

This article was originally published in *Building on 100 Years of Success: Proceedings of the 2006 International Thermal Spray Conference* (Seattle, WA), May 15-18, 2006, B.R. Marple, M.M. Hyland, Y.-Ch. Lau, R.S. Lima, and J. Voyer, Ed., ASM International, Materials Park, OH, 2006.

E. Moreau, C. Chazelas, G. Mariaux, and **A. Vardelle,** Laboratoire Sciences des Procédés Céramiques et Traitements de Surface, University of Limoges, Limoges, France. Contact e-mail: armelle@ensil.unilim.fr.

limit the heat load to the anode wall and, thus, its erosion. Various construction designs have been proposed in the literature or by torch manufacturers to reduce arc instabilities and anode erosion. For example, the axial movement of the arc root can be drastically reduced by using a segmented nozzle made up of a stack of several insulated segments and ending at an anode ring (Ref 4) or by using a very high gas flow that forces the arc to attach at the end of the nozzle (Ref 5). Both result in an increase in arc length and arc voltage and make it possible to use lower arc current or pure argon gas. The rotational movement may be restricted by using multi-arc torches or, as proposed recently by Dzulko et al. (Ref 6), by using a segmented anode made up of three segments forming a ring where the three arc roots are fixed. Although the construction of these various plasma torches and their functioning generally result in a more stable operating mode and longer anode life span, it requires more complex elements whose construction and maintenance involve a substantial initial and operating cost. Therefore, the study of how to achieve a "steady mode" of torch operation and an acceptable anode lifetime with conventional dc plasma torches is still warranted.

Experimental techniques based on the monitoring of arc voltage, sound, or light, have enabled the investigation of arc fluctuations (Ref 7-14) and a better understanding of the way it depends on the torch geometry and working parameters. Also, experimental (Ref 15) and numerical works (Ref 16, 17) dealing with the effect of arc fluctuations on particle behavior and coating formation have shown that a rather stable behavior is observed, thus, a better-quality coating is achieved (low porosity, low content of nonmelted particles, and high deposition efficiency) (Ref 18) when the time-evolution of the arc voltage exhibits a lower amplitude variation and a higher fluctuation frequency. In fact, the latter must be much higher than the time characteristics of particle heating and acceleration (Ref 19).

A reliable model that makes it possible to determine the movement of the anode spot and the time-variation of arc voltage, flow patterns, and heat flux to the anode wall may be a useful tool to correlate the torch parameters and the plasma jet fluctuations. However, such a model is still a challenge (Ref 20, 21) because it requires a detailed description of the interaction between the gas flow and the arc and of the nonequilibrium physics involved in the electrode boundary layers.

In this work, the authors present a time-dependent and three-dimensional model of arc dynamics that is under development at this laboratory. It is the same calculation method as that presented in Ref 16 and 17. However, different boundary conditions are used on the cathode end and anode wall and for arc breaking and restriking. Indeed, if the predictions of the previous study exhibited realistic variations with the operating torch parameters, they overestimated the arc voltage by 25% and gas temperature by 16%, bringing about an overestimation of the enthalpy input to the plasma jet (Ref 17).

In this paper, concentration is on the boundary conditions to be used to model the arc breakdown and restriking and the effect of arc current intensity on the thickness of the cold boundary layer and arc stability; torch operating conditions are used that make the arc operate in restrike mode, as shown by experimental observations (Ref 3).

2. Description of the Mathematical Model

2.1 Main Assumptions and Governing Equations

The model developed in this study is based on the following main assumptions:

- The gas flow inside the plasma torch is 3D, time-dependent, and laminar.
- The gas is treated as incompressible, as its Mach number is <0.3.
- Plasma is optically thin and in local thermodynamic equilibrium (LTE).
- The gas properties are temperature dependent.

Although the assumption of LTE is valid in the arc column, it is questionable in the electrode boundary layers where noticeable deviations from thermal and chemical equilibrium may occur. However, in this work, the objective is to achieve reliable predictions of the 3D and time-dependent interactions between the arc and gas flow; the model of the anode zone under development will be implemented in a computational fluid dynamics (CFD) code at a later stage.

On the basis of the foregoing assumptions, the fluid conservation equations and electromagnetic equations are written as follows:

Mass continuity equation

$$\frac{\partial \rho}{\partial t} + \mathrm{div}(\rho \vec{U}) = 0 \qquad \text{(Eq 1)}$$

where ρ is the gas mass density and $\vec{U}$ is the local instantaneous gas velocity.

Momentum conservation equation

$$\frac{\partial \rho \vec{U}}{\partial t} + \mathrm{div}(\rho \vec{U} \cdot \vec{U}) = \mathrm{div}\,\overleftrightarrow{\tau} - \mathrm{grad}\, p + \vec{j} \wedge \vec{B} + \rho \vec{g} \qquad \text{(Eq 2)}$$

where $\overleftrightarrow{\tau}$ is the stress tensor, p the pressure, $\vec{g}$ the gravity acceleration, $\vec{j}$ the current density vector, and $\vec{B}$ the magnetic induction vector. The term $j \wedge \vec{B}$ represents the electromagnetic Lorentz forces acting on the flow. This term is very sensitive to the curvature of the current lines (close to the cathode tip (Maecker effect) and the anode surface).

Energy conservation equation

$$\frac{\partial \rho h}{\partial t} + \mathrm{div}(\rho \cdot h \cdot \vec{U}) = \mathrm{div}\left(\frac{\kappa}{C_p} \cdot \mathrm{grad}\, h \right) + \vec{j} \cdot \vec{E} + S_{\mathrm{rad}} \qquad \text{(Eq 3)}$$

where h is the specific enthalpy, κ the gas thermal conductivity, C_p its specific heat, and $\vec{E}$ the electric field. S_{rad} stands for the radiation source term, and $\vec{j} \cdot \vec{E}$ represents the Joule heating.

Maxwell's equations must be solved to calculate the electromagnetic field. Simplified equations are used according to the global neutrality assumption and Ohm's law approximation as the current flow induced both by the arc motion and the electromagnetic field time-variation are small compared with that induced by the current conduction. The electric field $\vec{E}$ and the

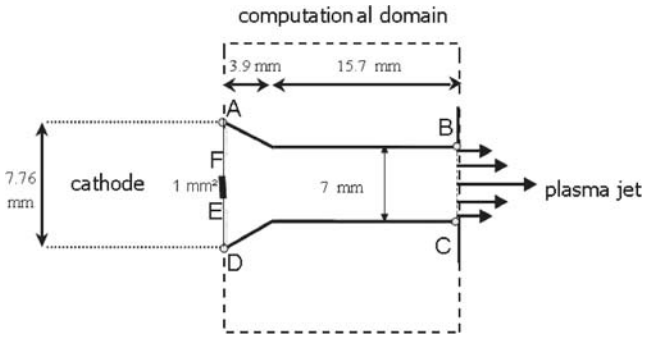

Fig. 2 Calculation domain

magnetic field $\vec{B}$ are determined from the electric potential Φ and the vector potential $\vec{A}$ through the following set of equations:

$$\mathrm{div}(-\sigma\, \vec{\mathrm{grad}}\, \Phi) = 0 \quad \text{(Eq 4)}$$

$$\vec{E} = -\vec{\mathrm{grad}}\, \Phi \quad \text{(Eq 5)}$$

$$\Delta \vec{A} = \mu_0 \vec{j} \quad \text{(Eq 6)}$$

$$\vec{j} = \sigma \vec{E} \quad \text{(Eq 7)}$$

$$\vec{B} = \vec{\mathrm{rot}}\, \vec{A} \quad \text{(Eq 8)}$$

Coupling between the electromagnetic and fluid equations is ensured by the dependence of the gas electric conductivity on temperature. The set of governing equations expressed in curvilinear coordinates is solved using the CFD code Saturne V1.1.1 based on the SIMPLEC algorithm (Ref 22) and uses nonstructured mesh grids.

2.2 Computational Domain and Boundary Conditions

The computational domain shown in Fig. 2 extends from the end of the cathode to the exit of the nozzle. The tungsten cathode [EF] is included in the computational domain as a flat surface of 1 mm^2. Boundary conditions for the flow and electromagnetic equations are shown in Table 1.

The plasma-forming gas enters the computational domain at a uniform temperature (300 K) and a vortex velocity profile. The latter is inferred from the calculation of the cold gas flow in the plasma torch, taking into account the entire domain of the arc chamber from the gas flow injection ring to the nozzle exit.

The heat flux at the anode surface resulting from gas conduction is spread over the entire surface of the nozzle wall, while the current flow contribution is located at the arc root attachment. In the present model, the heat flux transferred to the anode does not take into account the gas radiation and possible vaporization of the anode wall. It is hence expressed as:

$$-\frac{\kappa}{C_p}\frac{\partial h}{\partial n}\bigg|_w + j\left[W_s + \frac{5}{2}k_B T + V_a\right] = h_{\mathrm{overhall}}(T_w - T_\infty) \quad \text{(Eq 9)}$$

where h is the specific enthalpy, κ the gas thermal conductivity, C_p its specific heat, k_B the Boltzmann constant, and T the gas temperature.

The first term in the left-hand side of Eq 9 corresponds to the heat transfer due to the gas conduction, while the second term represents the energy released by the electrons entering the anode material. This term includes the heat transfer due to electron condensation (W_s), electron enthalpy flow, and anodic fall voltage, V_a. The electron condensation heat is expressed using the copper material work function ($W_s = 4.65$ eV), and the anode fall is set at 4 V (Ref 23).

The right-hand side of Eq 9 represents the heat flux removed by the cooling water. In this term, h_{overall} is the overall heat-transfer coefficient of the system that involves sequential conduction through the anode wall and convection to the water. T_w is the anode surface temperature, and T_∞ is the bulk temperature of the cooling fluid. The overall heat-transfer coefficient corresponds to a turbulent high-pressure flow in a pipe and is fixed to 0.2×10^5 W m^{-2} K^{-1}, as this value makes it possible to obtain a predicted torch thermal efficiency close to the actual one.

The metallic walls of the anode and cathode are considered as electric isopotentials. The electric potential is fixed at 0 at the cathode tip, while the anode potential Φ_0 results from calculation by postulating that the arc current is constant in the arc column.

2.3 Arc Breakdown and Restriking

In a plasma spray torch, the arc column is roughly parallel to the anode surface, and, thus, it may be considered that a cold boundary layer insulates electrically the arc column from the anode. Indeed, the electric conductivity of the main plasma-forming gases used in plasma spraying (argon, hydrogen, and nitrogen) is characterized by a critical temperature, ~7000 K, below which it is close to zero (Fig. 3).

A rather thick cold gas boundary layer (~1-2 mm) gives rise to the so-called restrike mode first described by Wutzke and Pfender (Ref 2). This mode is favored by the use of high gas flow rates and diatomic plasma gases. In this operation mode, the "tongue" that forms the current bridge between the main arc column and the anode wall is pushed forward by the gas flow in the outer layers of the main arc column until the cold boundary layer "electrically breaks," giving rise to a new path for the electric current and a new point of arc attachment. Thus, the arc voltage exhibits rather large fluctuations with a high mean value. This mode corresponds to a large range of plasma operating conditions used for plasma spraying and to those used in this study that combine high arc current and hydrogen content in the plasma-forming gas.

Much research has been done since the original work of Paschen in 1889 (Ref 25) that has become known as Paschen's Law, to develop a greater understanding of the mechanisms of electric arc breakdown. Paschen's Law reflects the Townsend breakdown mechanism in gases, that is, a cascading of secondary electrons emitted by collisions in the gap. It states essentially that the breakdown characteristics of a gap are a function (generally not linear) of the product of the gas pressure and the gap length, usually written as the breakdown voltage $V = f(pd)$, where p is the pressure and d is the gap distance. However, many factors affect the breakdown of a gap, such as radiation, gas temperature, and surface irregularities.

In this work, the breakdown process is modeled as follows (Fig. 4):

- The thickness δ of the boundary layer that covers the anode surface is defined by an electric conductivity lower than 150 Ωm^{-1}. The latter roughly corresponds to a temperature of 7000 K.
- The electric field between the edge of the arc column and the anode wall, $(\Phi_0 - V_A) / \delta$, is calculated in the whole boundary layer and compared with a critical field E_c, under which no breakdown process can occur.
- When this value is reached at a given location, a short circuit represented by a new arc attachment at the nozzle wall is initiated, while the previous arc attachment is extinguished. This process occurs generally within 1 μs (Ref 26).

A simple model is used for the ignition of the new arc root attachment. It consists of imposing an 8000 K gas column that connects the arc column to the anode wall, at the location where the electric field was found to be greater than E_c. If several locations satisfy the breakdown condition, the location corresponding to the maximum of the quantity $(\Phi_0 - V_A) / \delta$ is chosen. Also, the electrical potential at the anode wall is modified over 30 calculation time steps and set to the potential reached just before breakdown.

3. Results and Discussion

The calculations are performed with a plasma torch of 7 mm nozzle diameter and a high gas flow rate (60 slm) and a high hydrogen content (25%) in the plasma-forming gas, so as to favor the arc restrike mode. Two sets of operating conditions (Table 2) that differ in arc current intensity are considered.

3.1 Arc Ignition and Gas Flow Expansion inside the Torch Nozzle

After numerical simulation of arc ignition by imposing a 8000 K gas column of 1 mm thick connecting the tip of the cathode to the anode wall, both arc current and gas flow rate are linearly increased up to the nominal values during 400 calculation time steps (1 time step = 10^{-7} s). Figure 5 shows an example of the development of the arc inside the nozzle, from the first instant when the arc is ignited by the hot gas column (Fig. 5a), up to the instant where the first breakdown occurs (Fig. 5d).

The broadening of the arc column, mainly due to thermal effects (Joule heating, heat diffusion), and its stretching by drag forces exerted by the gas flow are clearly observed (Fig. 5); also, the rotational motion of the arc root on the anode wall principally controlled by the vortex injection of the plasma-forming gas and, to a slight extent, by the Lorentz forces acting on the arc root.

Table 1 Boundary conditions for the flow equations and the electromagnetic equations

	Enthalpy h, J/kg	Velocity V, m s^{-1}	Pressure p, Pa	Electrical potential Φ, V	Magnetic potential A, Wb m^{-1}
[AF], [DE] Inflow	$h = h_0$	Vortex profile	$\frac{\partial p}{\partial n} = 0$	$\frac{\partial \Phi}{\partial n} = 0$	$\frac{\partial A}{\partial n} = 0$
[EF] Cathode End	h(3200 K)	$V = 0$	$\frac{\partial p}{\partial n} = 0$	$\Phi = 0$	$\frac{\partial A}{\partial n} = 0$
[BC] Outflow	$\frac{\partial h}{\partial n} = 0$	$\frac{\partial v_z}{\partial n} = \frac{\partial v_n}{\partial n} = 0$	$p = p_0$	$\frac{\partial \Phi}{\partial n} = 0$	$A^{(n)} = A^{(n-1)}$
[AB], [DC] Anode wall	Eq 9	$V = 0$	$\frac{\partial p}{\partial n} = 0$	$\Phi = \Phi^{(n)}$	$\frac{\partial A}{\partial n} = 0$

n, current time step

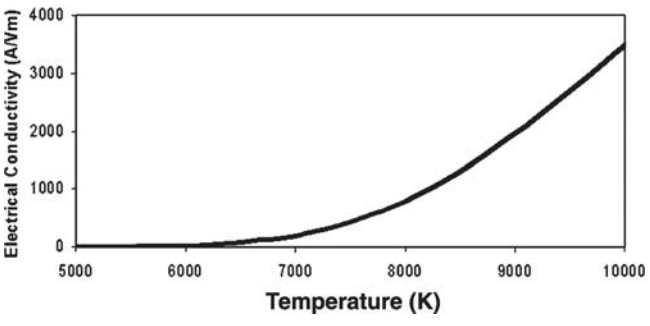

Fig. 3 Temperature dependence of the electric conductivity of Ar-H_2 (25% vol) gas mixture (Ref 24)

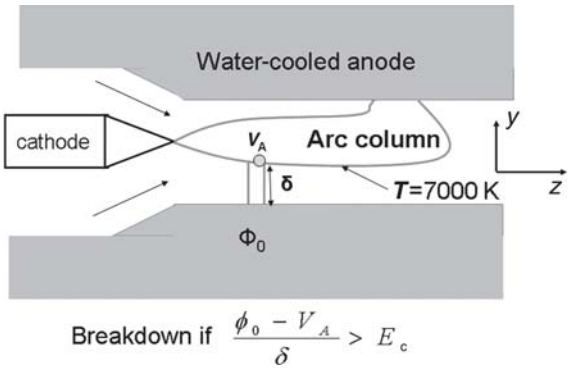

Fig. 4 Schematic description of the arc restrike location

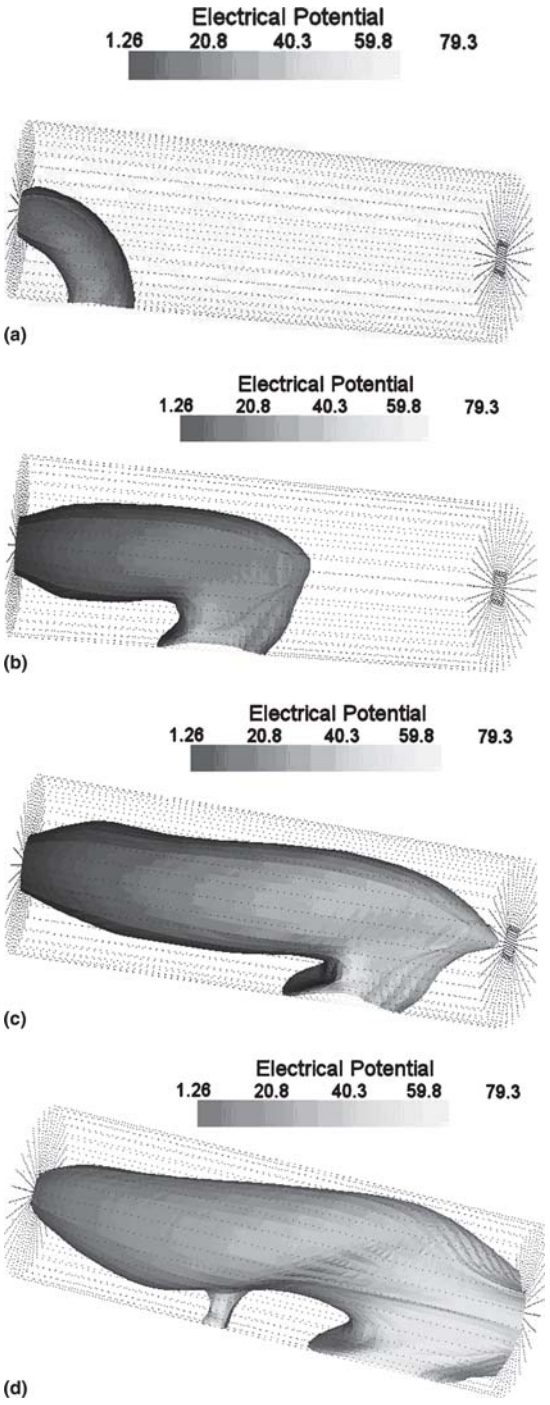

Fig. 5 Condition 1: ignition of the arc followed by the plasma flow expansion inside the torch nozzle (7000 K isotherm colored by the electric potential); in (d), a new arc root appears because the breakdown criterion has been satisfied.

3.2 Time-Evolution of Arc Voltage and Gas Characteristics at Torch Exit

Figure 6 shows the time-evolution of the predicted arc voltage for the operating condition 1. The critical electrical field is fixed at 0.5×10^5 V/m. It can be seen that the increase of the voltage ramps up to a peak value before decreasing rapidly. This

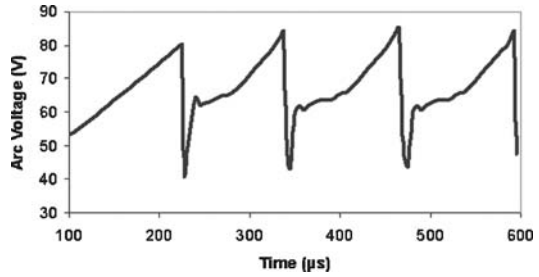

Fig. 6 Condition 1: time evolution of predicted arc voltage

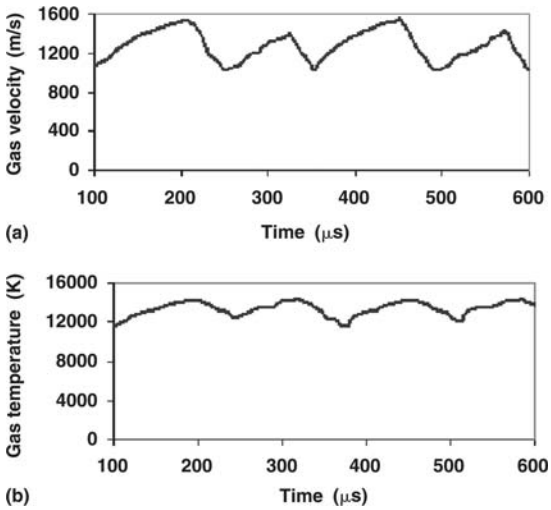

Fig. 7 Condition 1: (a) time evolution of the axial gas velocity and (b) temperature on torch axis at nozzle exit

Table 2 Plasma torch parameters

	Condition	
Parameter	**1**	**2**
Plasma-forming gas (slm)	Ar-H_2 (45:15)	
Gas mass flow rate (g/s)	1.25	
Arc current intensity (A)	600	400

cyclic arc behavior is characteristic of the restrike mode: the slope of the ramps indicates the rate at which the arc is stretched and lengthened by the flow

The arc lengthening is limited by an electrical breakdown through the cold gas boundary layer. Each breakdown is associated with a negative drop of the voltage δ_V. In the case shown in Fig. 6, the voltage drop was found to be ~40 V. The peak occurs at intervals of ~130 μs, i.e., at an average frequency, f, of ~7.5 kHz, while the actual arc frequency is ~5 kHz under the same experimental conditions. The predicted time-average torch voltage, $\overline{V}$, is found to be ~65 V, very close to the actual voltage of 60 V. It should be noted that the cathode and anode voltage falls are not involved in the calculated arc voltage because no specific models are considered for the electrode zones in this study.

The variations in the length and width of the arc column in the anode nozzle give rise to the time variation of the maximum gas temperature and velocity at the nozzle exit, as illustrated in Fig. 7. These fluctuations are in unison with the voltage fluctua-

tion that reflects the variation in arc column length. The maximum plasma flow temperature at the exit nozzle is 14,200 K, while the maximum plasma jet velocity, V_{max}, is 1550 m/s. As expected, the plasma jet velocity fluctuations ($\Delta U/U = 0.37$) are larger than those encountered for the temperature ($\Delta T/T = 0.21$). At temperature ranges between 9000 and 12,000 K, heat is stored in the gas species in the form of ionization energy that acts as a thermal inertia wheel and dampens the plasma temperature variation (Ref 24).

3.3 Effect of Arc Current on Cold Gas Boundary Thickness and Arc Frequency

Two simulations are carried out with the sets of operating conditions listed in Table 2. They use the same gas flow rate of 45 slm Ar and 15 slm H_2 but differ in arc current intensity of 400 and 600 A.

The results of Table 3 show that an increase in the arc current leads to the following observations:

- A decrease in the arc root spot size S_{spot}, delimited by the 7000 K isotherm, due to a rise in the electromagnetic forces that constrict the arc root. However, the predicted size is larger by an order of magnitude than the experimental value in the order of 1 mm^2 (Ref 14).
- A broader expansion of the arc column due to a more significant Joule heating and thus, a slight decrease in the cold gas boundary layer thickness δ_{mean}. The latter is still in good agreement with experimental values determined by Duan and Heberlein (Ref 1), satisfying the minimum thickness required for arc operation in restrike mode.
- A thinner cold gas boundary layer facilitating the arc breaking and leading to a lower amplitude of arc voltage fluctuation and, consequently, a higher arc fluctuation frequency. The latter agrees rather well with the actual voltage fluctuation usually ranging between 1 and 10 kHz for these operating conditions.
- A higher maximum gas velocity at the torch exit due to the higher enthalpy input to the gas and increase in Joule heating effect that acts on the gas expansion.
- A slight increase of the maximum temperature close to the anode surface in the connecting arc column as energy is essentially used to ionize the gas in this range of temperature. In addition, the thermal efficiency of the torch is about 55% and decreases slightly for a larger anodic spot.

3.4 Particle Acceleration and Heating

For powder particles, the plasma spraying process can be divided in two sequential stages, namely, penetration into the plasma flow and heating and acceleration up to the substrate. In fact, the particle trajectory and, consequently, its thermal and kinematic history in the plasma flow are essentially conditioned by the injection conditions and the gas flow fields at the instant when particles are injected into the gas, as it can be observed in Fig. 8. The latter shows the trajectories, in the *y-z* plane, of 25 μm alumina particles injected in to the plasma jet at different instants of the arc fluctuation period but with the same injection conditions: particles are located on the axis of the injector, and they leave the injector with an axial velocity of 20 m/s.

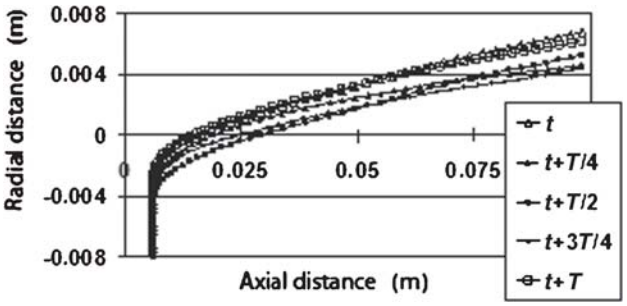

Fig. 8 Condition 1: trajectories of 25 μm particles injected at different instants of the fluctuation period with an injection velocity of 20 m/s (*y-z* plane)

Table 3 Effect of working parameters on plasma flow characteristics at the exit nozzle(a)

I, A	S_{spot}, mm^2	δ_{mean}, mm	$\Delta V/\bar{V}$	*f*, kHz	V_{max} output, m/s
400	19	1.8	0.57	5	1270
600	10	1.6	0.46	7.5	1550

(a) Torch nozzle diameter, 7 mm; total gas flow rate, 60 slm

Under the conditions of the study, the way the trajectory is affected by flow fluctuations depends essentially on the particle momentum with respect to the instantaneous momentum of the gas at the point where the particle penetrates the jet flow. The width of the particle spray jet, on impact at the substrate, is ~3.5 mm for 25 μm particles but is as large as 6.6 mm for 10 μm particles.

Fluctuation of the particle spray jet in the plasma flow will be limited by a decrease in the fluctuation amplitude of the plasma jet momentum. The latter depends both on gas velocity and temperature. When the torch operates in restrike mode, a "stable" treatment of the particles injected in the plasma jet requires that the reference characteristic time of the arc fluctuation is much lower than the reference characteristic time of the heating of particles.

Because the powders used in plasma spraying have a particle size distribution, some of them will be always affected by the arc fluctuation whatever the arc fluctuation frequency is. Therefore, it seems more efficient to act on the voltage fluctuation amplitude than on arc fluctuation frequency. Both are linked and are mainly governed by the thickness and the stability of the colder gas layer surrounding the plasma column. The thicker this layer, the higher the voltage jump and the lower the characteristic frequency. However, the latter must be high enough to prevent, or at least, to limit the anode erosion.

The issue is to find spraying conditions that ensure a stable thermal treatment of particles and the required particle parameters at impact to achieve a coating with reliable and reproducible properties. A reliable model of the transient conversion of the electrical energy into "plasma energy" inside the torch, linked with a model of plasma jet and particles outside the torch, makes it possible to investigate the effect of torch geometry, operating conditions for gas and particle injection, and, thus, to determine the conditions that result in a stable and optimized treatment of particles.

4. Conclusions

In this paper, a 3D, time-dependent model of the electric arc behavior inside a plasma spray torch operating under the so-called "restrike" mode has been presented. The model is based on simultaneous solution of the fluid flow and electromagnetic equations and uses the electric potential and magnetic vector potential to calculate the electric and magnetic fields.

The main conclusions drawn from the current study are the following:

- The model realistically predicts arc behavior and voltage fluctuation when the arc operates in the restrike mode; it also gives a realistic projection of the effect of the arc current variation on the arc behavior.
- It yields calculated values of cold gas boundary layer thickness, arc voltage, gas temperature, and torch thermal efficiency close to the experimental values.
- The model, at this stage of development, makes it possible to study the effect of the torch geometry and operating parameters on arc stability; i.e., arc frequency and variation in instantaneous voltage amplitude, when the arc operates in restrike mode.

However, the model still overestimates the size of the arc attachment at the anode wall. Implementation of a non-LTE model of the anode region, under development, should help to overcome these issues.

References

1. Z. Duan and J. Heberlein, Arc Instabilities in a Plasma Spray Torch, *J. Therm. Spray Technol.,* 2002, **11,** p 44-57
2. S.A. Wutzke, E. Pfender, and E.R.G. Eckert, Study of Electric Arc Behavior with Superimposed Flow, *IAAA J.,* 1967, **5**(4), p 707
3. C. Chazelas, J.F. Coudert, and P. Fauchais, Arc Root Behavior in Plasma Spray Torch, *IEEE Trans. Plasma Sci.,* 2005, **33**(2) p 414-420
4. J. Zierhut, P. Haslbeck, K.D. Landes, G. Barbezat, M. Müller, M. Schutz, Triplex: An Innovative Three-Cathode Plasma Torch, *Proc. 15th Int. Spray Conf.,* 1998 (Nice, France), ASM International, 1998, p 1375-1378
5. P. Fauchais, Understanding Plasma Spraying, *J. Phys. D: Appl. Phys.,* 2004, **37,** p R86-R108
6. M. Dzulko, G. Forster, K.B. Landes, and K. Nassenstein, Plasma Torch Developments, *Proc. Int. Thermal Spray Conf.,* May 2-4, 2005 (Basel, Switzerland)
7. S.A. Wutzke, "Conditions Governing the Symptomatic Behavior of an Electric Arc in a Superimposed Flow Field," Ph.D. thesis, University of Minnesota, 1967
8. R. Hartmann and J. Heberlein, Quantitative Investigations on Arc-Anode Attachments in Transferred Arcs, *J. Phys. D Appl. Phys.,* 2001, **34**(19), p 2972-2978
9. Z. Duan, "Investigation of Plasma Instabilities in a Spray Torch," Ph.D. thesis, University of Minnesota, 2000
10. J. Hlina and V. Nénicka, Identification of Local Oscillations in a Plasma Jet, *Prog. Plasma Process. Mater.,* 1999, p 333-337
11. M. Vysholid, "Arc Voltage Fluctuations in a Plasma Torch," Masters thesis, University of Minnesota, 2003
12. J.F. Brilhac, B. Pateyron, J.F. Coudert, and P. Fauchais, Study of the Dynamical and Static Behaviour of DC Vortex Plasma Torches, *Plasma Chem. Plasma Process.,* 1995, **15**(2), p 255-277
13. J.M. Sobrino, J.F. Coudert, and P. Fauchais, Anodic Arc Root Behavior of a Transferred Arc, *Proc. 12th Int. Symp. Plasma Chemistry,* Aug 8-11, 1995 (Minneapolis, MN), Vol III, International Plasma Chemistry Society, 1995, p 1455-1460
14. D. Rigot, "Electrode Erosion in a Plasma Spray Torch," Ph.D. thesis, University of Limoges, 2004, in French
15. J.F. Bisson, B. Gautier, and C. Moreau, Effect of Plasma Fluctuations on in-Flight Particle, *J. Therm, Spray Technol.,* 2003, **12,** p 38-43
16. C. Baudry, A. Vardelle, and G. Mariaux, 3-Dimensional and Time-Dependent Model of the Dynamic Behavior of the Arc of a Plasma Spray Torch, Thermal Spray 2004: Advances in Technology and Application, May 10-12, 2004 (Osaka, Japan), ASM International, p 1129
17. C. Baudry, A. Vardelle, G. Mariaux, M. Abbaoui, and A. Lefort, Numerical Modelling of a DC Non-Transferred Plasma Torch, *High Temp. Mater. Process.,* 2005, **9**(1), p 1-16
18. L. Leblanc and C. Moreau, The Long-Term Stability of Plasma Spraying, *J. Therm. Spray. Technol.,* 2002, **11**(3), p 380-386
19. A. Vardelle, P. Fauchais, B. Dussoubs, and N.J. Themelis, Heat Generation and Particle Injection in Thermal Plasma Torch, *Plasma Chem. Plasma Process.,* 1998, **18**(4), p 551-578
20. H.P. Li, J. Heberlein, and E. Pfender, Three-Dimensional Modelling of Non-Equilibrium Effect in a Transferred DC Arc Plasma with Lateral Gas Blowing, *Proc. 17th Int. Symp. Plasma Chemistry,* Aug 7-12, 2005 (Toronto, Canada) International Plasma Chemistry Society, 2005
21. V. Colombo and E. Ghedini, Time-Dependent 3-D Simulation of a DC Non-Transferred Arc Plasma Torch, *Proc. 17th Int. Symp. Plasma Chemistry,* Aug 7-12, 2005 (Toronto, Canada) Internatioal Plasma Chemistry Society, 2005
22. F. Archambeau, Code-Saturne: A Finite-Volume Code for the Computation of Turbulent Incompressible Flows, *Int. J. Finite Volume,* 2004 **1**(1), (Feb)
23. J. Jenista, J. Heberlein, and E. Pfender, Numerical Model of the Anode Region of High-Current Electric Arcs, *IEEE Trans. Plasma Sci.,* 1997, **25**(5), p 883-890
24. M. I. Boulos, P. Fauchais, and E. Pfender, *Thermal Plasmas: Fundamentals and Applications,* Plenum Publishing Corporation, Vol 1
25. F. Paschen, Über die zum Funkenübergang in Luft, Wasserstoff and Kohlensaűre bei verschiedenen Drucken erforderliche Potentialdifferenz, *Ann. Phys.,* 1889, **37,** p 69-96
26. J.F. Coudert, C. Chazelas, D. Rigot, and V. Rat, From Transferred Arc to Plasma Torch, *J. High Temp. Mater. Process.,* 2005, **9**(2), p 155-164